NISTIR 5192

In Situ Burning of Oil Spills: Mesoscale Experiments

William D. Walton

September 1993

Building and Fire Research Laboratory
National Institute of Standards and Technology
Gaithersburg, MD 20899

U.S. Department of Commerce
Ronald H. Brown, *Secretary*
Technology Administration
Mary L. Good, *Under Secretary for Technology*
National Institute of Standards and Technology
Arati Prabhakar, *Director*

Prepared for:
U.S. Department of Interior
Bruce Babbitt, *Secretary*
Minerals Management Service
Technology Assessment and Research Branch
Herndon, VA 22070

TABLE OF CONTENTS

LIST OF TABLES

LIST OF FIGURES

In Situ Burning of Oil Spills: Mesoscale Experiments and Analysis

William D. Walton
Building and Fire Research Laboratory,
U.S. National Institute of Standards and Technology

ABSTRACT

A series of six mesoscale experiments were performed to measure the burning characteristics of Louisiana crude oil on water in a pan. These included one - 6 m square and five - 15 m square burns. Results of the measurements for burning rate and smoke emissions are compared to those from previous burns of various scales. The burning rate as indicated by the regression rate of the oil surface was found to be 0.062 ± 0.003 mm/s for both the 6 m and 15 m square pan fires. Smoke particulate yields from the 15 m square fires were found to be approximately 11% of the oil burned on a mass basis.

Key words: burning rate, crude oil, fire tests, heat release rate, oil spills, particle size distribution, plumes, pool fires, smoke yield

1.0 INTRODUCTION

In-situ burning of spilled oil has distinct advantages over other countermeasures. It offers the potential to convert rapidly large quantities of oil into its primary combustion products, carbon dioxide and water, with a small percentage of smoke particulate and other unburned and residue byproducts. Burning of spilled oil from the water surface reduces the chances of shoreline contamination and damage to biota by removing the oil from the water surface before it spreads and moves. In situ burning requires minimal equipment and less labor than other techniques. It can be applied in areas where many other methods cannot due to lack of response infra-structure and/or lack of alternatives. Oil spills amongst ice and on ice are examples of situations where practical alternatives to burning are very limited. Because the oil is mainly converted to airborne products of combustion by burning, the need for physical collection, storage, and transport of recovered fluids is reduced to the few percent of the original spill volume that remains as residue after burning.

Burning oil spills produces a visible smoke plume containing smoke particulate and other products of combustion which may persist over many kilometers downwind from the burn. This fact gives rise to public health concerns, related to the chemical content of the smoke plume and the downwind deposition of particulate, which need to be answered. Air quality is also affected by evaporation of large oil spills that are not burned. Volatile organic compounds (VOC) including benzene, toluene, and xylene and polycyclic aromatic hydrocarbons (PAH) are found in the air downwind of an evaporating crude oil spill. Laboratory measurements are useful to determine the types of chemical compounds that can be expected from large oil spill burns or the evaporation of the spill. To determine the rate of emissions and the transport of the chemical compounds from a burning or evaporating spill, mesoscale experiments have been conducted outdoors using a 15 m square pan. In these experiments a layer of crude oil was discharged onto the surface of a salt water pool and burned.

2.0 BACKGROUND

Extensive experimental studies to quantify the capabilities of in situ burning began in 1983 at the Oil and Hazardous Materials Simulated Environmental Test Tank (OHMSETT) facility in Leonardo, New Jersey under joint funding from the Minerals Management Service (MMS), U.S. Coast Guard (USCG), Environmental Protection Agency (EPA), and Environment Canada (EC). Results showed that 50 to 95 percent of all of the oils tested could be removed from the water surface by burning [1-4].

Based upon the success of these research efforts, a joint MMS and EC in situ burning research program continued in 1985. This research program was designed to study how burning large oil spills would affect air quality by quantifying the products of combustion and developing methods to predict the downwind smoke particulate deposition. Initially, laboratory experiments were conducted by the Center for Fire Research, now the Building and Fire Research Laboratory, at the National Institute of Standards and Technology (NIST) [5-8]. This work sought to quantify the processes involved in oil spill combustion on water and included measurements of smoke production and prediction of smoke dispersal. Technical support from EC allowed the study to be broadened to include chemical analysis of the oil, oil residue, and oil smoke.

Mesoscale outdoor burns were conducted to verify that the favorable results obtained in the laboratory would apply to burns at a scale approaching that expected to be used in oil spill mitigation. New instrumentation techniques were developed to conduct measurements during the mesoscale burns and have been improved and refined in subsequent mesoscale and large indoor burns [9-13].

3.0 EXPERIMENTAL FACILITY

To understand the important features of in situ burning it is necessary to perform both laboratory and mesoscale experiments. In addition, burns of intentional releases of crude oil at sea at the scale of an anticipated response will be necessary to measure the effects of increased burn area, waves, and movement of oil over the water in a boom, which have not been assessed in laboratory and mesoscale experiments. In this research program there is a continuing interaction between findings from measurements on small fire experiments performed in the controlled laboratory environments and large fire experiments at facilities such as the USCG Fire Safety and Test Detachment in Mobile, Alabama where outdoor mesoscale liquid fuel burns in large pans are possible.

3.1 Mesoscale configuration

The mesoscale burns of crude oil were carried out under the direction of NIST at the United States Coast Guard Fire and Safety Test Detachment facility on Little Sand Island in Mobile Bay, Alabama. Little Sand Island is approximately 0.2 km^2 in size and includes three decommissioned ships docked in a lagoon. The ships and facilities on the island have been used for a wide variety of full-scale marine fire tests. Figure 1 is a photograph of a burn in progress, and figure 2 is a plan view of the portion of the island used for the mesoscale oil spill burns.

The burns were conducted in a nominal 15 m square steel burn pan constructed specifically for oil spill burning. The burn pan was 0.61 m deep and was constructed with two perimeter walls approximately 1.2 m apart forming an inner and outer area of the pan. The base of the pan was located on ground level. The inside dimensions of the inner area of the pan were 15.2 m by 15.2 m. The two perimeter walls were connected with baffles and the space between the walls, which formed the outer area of the pan, was filled with water from Mobile Bay during the burns. The inner area of the pan was filled with approximately 0.5 m of bay water and the crude oil was added on top of the water.

The crude oil used in the mesoscale burns was obtained from an oil storage facility in Louisiana. The oil originated from wells in the Louisiana area and is thus referred to as Louisiana crude oil. The oil was 85.79% carbon, 13.25% hydrogen, and 0.41% sulfur by mass as measured by a commercial testing laboratory. Crude oil was pumped to the burn pan via an underground pipe. A vertical section of the oil fill pipe penetrated the base of the pan and terminated in a fitting to disperse the oil horizontally below the water level.

Two different primary burn areas were used in the series. These areas consisted of the full inner pan with an area of 231 m^2 and a partial pan area of 37.2 m^2. The partial pan area was achieved by partitioning a corner of the inner pan with two 6.1 m sections of fire resistant boom.

A total of 6 mesoscale burns were conducted. Table 1 gives the size and areas for the mesoscale burns. An effective diameter was calculated for both of the rectangular burn areas. The effective diameter is the diameter of a circle with the same area as the rectangular burn area used.

3.2 Instrumentation

The fixed position instrumentation in the burn pan consisted of a manometer and pressure transducer to measure the liquid level in the pan. Since the oil and the water in the pan had different densities, a correction was applied to determine the thickness of the oil layer during the burn. A copper tube was connected to the inner pan through a pipe penetrating the inner and outer walls of the pan. The tube ran

underground to the instrumentation building and connected to a liquid manometer and a pressure transducer. The output from the pressure transducer was recorded every two seconds on a computerized data acquisition system.

A portable array of 8 - 0.5 mm diameter bare-bead thermocouples 76 mm apart was used to determine the temperature of the water in the inner pan at two locations on opposite sides of the pan before and after the burns.

Measurements of atmospheric conditions were made with two ground based and one airborne weather stations. The first ground based station was located 58 m at 255° from the southwest corner of the burn pan and 2.1 m above the ground. The second ground based weather station was located 49 m at 240° from the southwest corner of the burn pan and 2.6 m above the ground. Both ground stations consisted of a thermistor to measure temperature, a propeller on vane anemometer to measure wind direction and speed, and a capacitive relative humidity sensor. In addition the first weather station had a silicon photodiode pyranometer to measure incident solar radiation. Atmospheric data from the first ground based weather station were recorded every 30 s and from the second station every 32 s with a computerized data acquisition system. The airborne weather station was connected to a helium filled miniblimp which was tethered approximately 30 m above the ground and located approximately 50 m from the pan upwind of the fire and well away from the effects of the fire plume. The airborne weather station consisted of a thermistor to measure temperature, a cup anemometer to measure wind speed, an electronic compass to measure wind direction, and a pressure transducer to measure barometric pressure. Data from the airborne weather station were transmitted via radio to a ground based computerized data collection system every 20 s.

The ground based measurements consisted of gas samples which were collected at regular intervals both up- and downwind of the fire. These samples were analyzed for carbon dioxide concentration on site after the burn.

Additional ground based measurements were made by other agencies and consisted of both real time measurements and samples collected for laboratory measurement. The real time measurements made both up- and downwind of the fire included total particulates and carbon dioxide, and sulfur dioxide concentrations. Filter samples were collected both upwind and downwind of the fire and analyzed in the laboratory for PAH and VOC concentrations. Samples of the fresh oil before the burn, oil residue after the burn, and water in the burn pan after the burn were collected for analysis in the laboratory. The results of these ground based measurements and the laboratory analysis will be presented by the agencies which collected the data and are not given in this paper.

Airborne samples were collected for both laboratory analysis and analysis on the ground immediately following the burns. Table 2 gives a list of the airborne samples taken. The sampling packages were suspended approximately 60 m below a 9.0 m long 3.3 m diameter tethered helium filled miniblimp. The miniblimp was positioned downwind from the fire with the sampling package centered in the smoke plume. The elevation and downwind position of the sampling package varied with each burn as a function of the plume position. Typically, sampling packages remained in the plume for over 1000 seconds which permitted an adequate sample to be collected and allowed the natural fluctuations in the plume to be averaged. Since the lift capacity of the miniblimp was limited, depending on the elevation of the plume anticipated prior to the burn, from 1 to 4 sampling packages were deployed at a time.

3.3 Burn procedure

Prior to pumping crude oil into the pan, water was pumped into the outer pan so that the water level was nearly to the top of the pan. Water was also pumped into the inner pan so that the water surface level was approximately 110 mm below the top of the pan. The distance from four reference points at the top of each side of the pan to the surface of the water in the inner pan was measured and recorded. The temperature profile of the water in the inner pan was measured at two locations on opposite sides of the pan. A water sample from the inner pan was analyzed for salinity.

The crude oil was stored on a barge which was brought to the site prior to each burn. Oil was pumped through a flexible hose from the barge through the underground piping system and into the pan. The approximate quantity of oil delivered to the pan was monitored with an in-line flow meter. When the quantity of oil delivered to the pan approached the desired quantity, compressed air was pumped from the barge to purge the flexible hose. The barge was then disconnected from the flexible hose and the barge departed the site. The distance from the surface of the oil to the fixed reference point at the top of the pan was recorded and an oil sample was taken. The fixed position and ground based instrumentation and data recording were started and the oil was easily ignited with an extended propane torch. Video cameras were used to record the burn.

When the fire was out, the temperature profile of the water in the inner pan was measured at two locations on opposite sides of the pan. The distance from the surface of the water/oil residue to the fixed reference point at the top of the pan was recorded on the four sides of the pan. The residue was collected with absorbent material and placed in drums for disposal. The quantity of residue was estimated from the volume of the drums filled taking into account the absorbent material and water collected. After four of the burns (1105, 1107, 1109, and 1110), there was a greater quantity of residue than could be readily collected in two or three drums. It is estimated that there was two to three times the quantity of residue then found in the earlier burns due to variations in the extinction process. In these cases to aid in the clean-up, a small quantity of diesel fuel was poured on the residue after it had cooled and the diesel and burn residue mixture was ignited. This procedure was repeated two times for burns 1109 and 1110 until the residue had been reduced to a quantity which could be placed in two drums. The residue was then collected and measured.

4.0 EXPERIMENTAL RESULTS

Table 3 gives a summary of the ground and table 4 the airborne meteorological conditions measured during each of the mesoscale burns. The values in the table are averages over the time from ignition to extinction. Wind directions are the direction from which the wind originates with 0° being north. Also shown in these tables are the maximum and minimum values measured during the burn. In table 3 the results for the two ground weather stations are given for each burn. There is generally good agreement between the two stations although there is a consistent difference in the atmospheric pressure. Since the pressure transducer in the weather station in the first column was most recently calibrated it is assumed to be accurate. Although the meteorological conditions varied during the burns, the burns were of relatively short duration and the averages are representative of the actual conditions. The airborne weather data was collected at an elevation of approximately 30 m and previous measurements showed the meteorological conditions to be generally uniform above 20 m [13].

4.1 Burning rate

The burning of the crude oil was observed to take place in four distinct phases. The four phases were; 1) spreading, 2) steady burning, 3) steady burning with boiling of the water below the oil layer, and 4)

transition to extinction. The spreading phase lasted from 80 to 180 s as flames spread over the surface from the single ignition point on the upwind side of the pan to cover the entire fuel surface. Once the entire oil surface was covered with flames, the burning continued at a steady rate until the water below the oil surface began to boil. The onset of boiling was characterized by a noticeable increase in fire generated sound which resembles sizzling and bubbles breaking through the oil surface. During boiling the burning rate increased to a steady rate which was greater than the rate prior to boiling. When the fuel was nearly consumed, the fire began a transition to extinction. This was characterized by areas of the oil surface with no visible flames. Frequently, there were oscillations in the burning behavior with increased and decreased burning area and transition to and from boiling. The burning area decreased toward the downwind side of the pan until extinction. A brief chronology of the observed burning behavior for each of the burns is given in table 5.

The initial volume of oil was estimated using the liquid surface measurements taken before the oil was added and after the oil was added. Table 6 gives the initial volume of oil, the volume of residue collected, the volume of oil consumed by burning and the percentage of the initial volume of oil consumed by burning. In the cases where the residue was burned before cleanup the number and duration of the residue burns is shown. The oil consumed is the total oil consumed during both the primary and residue burns.

The burning rate or the rate at which the oil was consumed during burning was estimated from the liquid level in the pan as measured by the pressure transducer. The output of the pressure transducer was calibrated in salt water and converted to oil depth using the specific gravity of the oil. The specific gravity of the oil was 0.846 ±0.001 as measured using the mechanical oscillator technique with an accuracy of ±0.001. The salt content of the water in the pan was measured before each test using the sodium ion electrode method with an accuracy of ±0.01 %. The salt concentration in percent NaCl and specific gravity of the water in the pan for each burn is given in table 7. The oil surface regression rate was calculated using a least squares linear fit of the pressure transducer output over the time from full pan involvement to the beginning of extinction. The data showed no difference in the burning rate before and during boiling.

The specific mass burning rate (rate of mass loss per unit area) was calculated from the surface regression rate and the density of the oil. The heat release rate was determined by multiplying the mass loss rate by the effective heat of combustion for the crude oil (41.9 MJ/kg) [13].

Table 8 shows the burning and surface regression rates and the observed burn times. Table 9 gives the same information in customary units. Figure 3 is a graph of the surface regression rate as a function of the effective burn diameter. From this graph it appears that for the range of diameters used in the mesoscale burns there is no dependency of surface regression rate on burn area. The mean value is 0.062 ± 0.003 mm/s. The mean value for the burning rate per unit area is 0.052 ± 0.002 kg/s/m^2 (5.4 ± 0.2 gal/hr/ft^2) and for the heat release rate per unit area is 2180 ± 100 kW/m^2. The scatter in the regression, burning and heat release rates was due in part to the variable nature of the burns. The wind direction and speed contributed to the wide variation in extinction behavior observed although it did not appear to affect the average burning rate. In mesoscale burns 1103 and 1106 the wind corralled the remaining fuel in a corner of the pan as the fire approached extinction allowing almost all the fuel to be consumed in a small area fire that burned in the corner. These burns are thought to be most representative of results expected from oil burning in a towed boom. Like the wind corralling fuel into the corner of the mesoscale pan, the motion of the towed boom over the water and wind forces would corral oil in the apex of the boom allowing all the oil to be consumed before fire extinction.

In previous experiments [13] the oil surface regression rate was determined from the liquid level measurements by dividing the quantity of fuel consumed by the burn time from full pan involvement to

the beginning of extinction. Table 10 gives the oil surface regression rate determined from the pressure transducer and the measurements of the oil surface level. The average regression rate determined from the liquid surface measurements of 0.064 mm/s is within 5% of the average rate determined from the pressure transducer. The regression rates calculated from the pressure transducer measurements show less variation than the rate calculated from the liquid surface measurements. This comparison indicates that the regression rates calculated from the pressure transducer measurements are more representative of the actual regression rates.

4.2 Smoke yield

The smoke production from a fire may be expressed in terms of a smoke yield Y_S which is defined as the mass of smoke particulate m_P produced from burning a fuel mass m_F, as:

$$Y_S = \frac{m_P}{m_F} \tag{1}$$

The mass of carbon in the fuel that is consumed by burning is equal to the mass of carbon in the smoke plume.

$$m_{C,Smoke} = m_{C,Fuel} \tag{2}$$

Three assumptions are made in the analysis. The first is that the smoke particulate is predominately carbon. Previous laboratory measurements [10] have shown that the organic carbon fraction of smoke from crude oil pool fires is not greater than 10 percent before there is any boiling in of supporting water sublayer. The remainder of the smoke contains greater than 90 percent elemental carbon. Thus the total carbon content which includes the elemental carbon and the carbon contained in the organic fraction is well over 90 percent of the content of the smoke. Based on this evidence, for the purpose of the smoke yield analysis the smoke particulate is considered to be pure carbon. The second assumption is that samples are collected over a suitable time period to average out natural fluctuations in the fire and plume. In the mesoscale tests and laboratory tests, samples are drawn over a period of 600 to over 1000 seconds. This is deemed sufficient to represent the average burning conditions for the fires. The third assumption is that no preferential separation of smoke particulate and combustion gases occur in the smoke plume up to the point where the sample is taken. In all field measurements, and unconfined laboratory burns, the smoke yield measurement is made close to the source where the smoke and gaseous combustion products move in a well formed smoke plume. Combining equations (1) and (2) and taking into account the three assumptions above yields:

$$Y_S = \frac{m_P}{m_{C,Smoke}} \frac{m_{C,Fuel}}{m_F} \tag{3}$$

To evaluate the above ratio, a known volume of smoke is drawn though a filter and the gaseous portion collected in a sample bag. The mass of carbon in the smoke is equal to the mass of carbon in the smoke particulate plus the mass of carbon in the CO_2 and CO in the smoke. In both the laboratory burn and the mesoscale burns, the concentration of CO in the gas samples were negligible. The smoke particulate mass is determined by weighing the filter. The mass of the carbon in the gas is the grams of carbon per mole of CO_2 (and CO) times the moles of gas sample times the difference in the volume fraction of CO_2 (and

CO) in the sample and the background. The volume fraction of CO_2 in the sample and the background were determined using a gas chromatograph. The mass of carbon in the smoke is:

$$m_{C,Smoke} = m_P + 12\frac{g}{mole}n(\chi^S_{CO_2}-\chi^B_{CO_2}) + 12\frac{g}{mole}n(\chi^S_{CO}-\chi^B_{CO}) \quad (4)$$

The moles of gas in the smoke sample were calculated using the ideal gas law.

$$n=\frac{PV}{RT} \quad (5)$$

where:
n = moles of gas (mol)
P = atmospheric pressure (kPa)
V = total volume of gas sampled (L)
R = gas constant 8.314 (kPa L/K g mol)
T = ambient temperature (K)

As tested in the laboratory, the flow controllers on the pumps used provide nearly constant mass flow over the range of temperatures experienced in the fire plume so the pressure and temperature in the equation above were taken at the location where the pump flows were calibrated.

The ratio $m_{C,Fuel}/m_F$ is evaluated by determining the elemental carbon mass fraction in the fuel. From the elemental analysis of the Louisiana crude oil, this value is 0.8579.

Combining equations (3) and (4) yields the expression for smoke yield in terms of the measured quantities.

$$Y_S=\frac{m_P\ (m_{C,Fuel}/m_F)}{m_P + 12\ n\ (\Delta\chi_{CO_2} + \Delta\chi_{CO})} \quad (6)$$

where: $\Delta\chi_{CO_2}$ = difference between the volume fraction of CO_2 in the sample and the background
$\Delta\chi_{CO}$ = difference between the volume fraction of CO in the sample and the background

In the field, smoke was drawn by a battery operated pump through a pre-weighed filter which collected the particulates. The gas passed through the pump to a micrometer adjusted flow control valve and exhaust orifice which metered a portion of the gas flow to a 5 liter sample collection bag. The flow through the filter was measured with a bubble flowmeter prior to each use. The filter samples were weighed on a precision balance before and after the burn and the concentration of CO_2 in the sample collection bag was determined using a gas chromatograph. In the mesoscale burns, the sampling package was suspended below a tethered miniblimp which was manually maneuvered from the ground and held in the smoke plume downwind of the fire. The altitude and range from the fire are given in table 2. A radio controlled switch was used to start and stop the pump remotely as the sampling package was carried into and removed from the fire plume [11]. The sample collection times were nominally 1000 seconds.

Smoke yields from the mesoscale burns are given in table 11. The smoke yields are shown in figure 4 along with measurements from previous burns[14]. From figure 4 it can be seen that smoke yield is dependent on fire diameter. The yield is generally lower for smaller diameter fires. In small diameter

fires the air which is entrained around the fire perimeter more readily mixes with the fuel resulting in more complete combustion and a lower smoke yield.

The smoke yield from the partial pan burn 1103 is distinctly higher than the yields from the other burns. This with the data from the previous burns suggests that either the smoke yield is higher for this diameter fire or that there is a characteristic of the 6.88 m diameter fires that has not been accounted for.

4.3 Particle size distribution

Particulate size is an important health consideration and also impacts the dynamics of smoke settling. Particulates having an aerodynamic effective diameter less than 10 μm are considered respirable [15] and may be drawn into the lungs with normal breathing. In general small particle sizes have the greatest resistance to settling and can be expected to be carried much further from the burn site than larger particles. In addition to the overall particulate yield from the crude oil fires, it is therefore important to have some knowledge about the particulate aerodynamic size distribution.

There are no means to directly translate the observed irregular shape of smoke particles [11] into aerodynamic effective diameters. The aerodynamic effective diameter of a particle is defined as the diameter of a smooth spherical particle with a unit density of 1000 kg/m^3 (1 g/cm^3) that has the same settling velocity in air. Therefore, the aerodynamic effective diameter of a particle depends on the size, shape and density of the particle. Cascade impactors measure particle size distribution by the amount of particulate deposited on a series of plates. The particulate laden air is drawn through the cascade impactor which consists of a series of stages each having a nozzle and plate. Aerodynamic forces determine the size ranges that will be deposited on the plate in each stage and the sizes that will pass through to other stages downstream. The fraction of the total deposition collected by each stage of the device determines the distribution of the aerodynamic effective diameter of the particles. The small and light weight commercial impactors used in this study contained 8 stages. For cases where a small quantity of particulate is expected, some of the stages may be removed. Each stage of the impactor is characterized by its cutpoint diameter. The cutpoint diameter is the aerodynamic effective diameter that is collected with 50 percent efficiency. Ideally the cutpoint diameter represents the largest diameter particle which will not pass to the next stage but in practice some larger particles do move to the next stage. The cutpoint diameter is a function of the flow rate through the instrument and decreases with increasing flow rate.

The impactor was operated at a flow rate of 0.033 L/s with 8 stages and a back-up filter. Table 12 shows the cutpoint diameters for each of the stages in the instrument and the back-up filter [16]. Figure 5 shows the cumulative size distribution of smoke particulate from a 17.2 m effective diameter mesoscale fire (1110).

4.4 Water temperature

Temperatures were measured in the water before and after some of the burns with a portable thermocouple array and in both the oil and water during some of the burns with the fixed thermocouple array in order to quantify the thermal effects of burning oil on the water column. Tables 13, 14 and 15 give the water temperatures measured with the portable thermocouple array. The tables give the time before ignition or after extinction at which the measurements were made and the location of the measurements. All measurements were made approximately 600 mm from the wall of the pan. For the partial pan burn the measurements were made just outside of the boom burn area on the North and West sides of the pan. For the full pan burns the measurements were made at the center of the north and south side of the pan.

The thermocouple array was placed on the bottom of the pan and the elevation of the measurement points is with respect to the bottom of the pan. A temperature measurement was made at the water surface and the approximate elevation of the water surface is indicated in parentheses. The variation in the elevation of the water is primarily due to the uneven bottom of the pan and to a lesser extent the movement of the pan during the burn and wind induced movement of the water. As a result, although the vertical measurement locations reflect the local elevation within ±2 mm, the difference between the elevation measured and the elevation of a level plane is estimated to be within ±12 mm.

The water temperature measurements with the portable thermocouple array show that the water temperature in the pan was uniform with depth and uniform across the pan. The water temperature in the burn area after the fire generally increased 5-40°C within 35 mm of the surface, 1-4°C, 70-115 mm below the surface, and increased 2°C or less at distances greater than 145 mm below the surface. Temperatures in the oil residue were 10-30°C higher than the expected water temperature at the same location. In most cases the water temperatures after the fire reflect the influence of the wind direction on the flames with the temperatures being hotter on the downwind side.

These water temperatures are in agreement with prior measurements and analysis [17] which indicate the thermal penetration rate into the water is slow when compared to the oil surface regression rate and high temperatures in the water are limited to 35-50 mm below the surface. The thermal penetration of the water is nearly the same for longer burns with thicker oil layers since the temperature in the water does not begin to rise significantly until the burning oil surface nears the water surface.

4.4 Ground level carbon dioxide concentration

Ground level measurements of CO_2 concentration were made at two locations directly downwind of each of the burns and at one location upwind of burns 1103 and 1105. At regular time intervals air samples at each of the sampling locations were rapidly pumped into a gas sample collection bag and smoke conditions at the sample location noted. The samples included one prior to the start of the burn and one after the completion of the burn to determine the background conditions. After the burn was completed the samples were analyzed at the burn site using a portable gas chromatograph. The chromatograph was calibrated each day using a reference gas with a known CO_2 concentration of 528 ppm.

Tables 16 through 21 show the downwind ground level measurements of CO_2 concentration and the observations at time the gas sample was taken. The times given are from ignition. Although the observation of smoke is subjective, the observer noted whether the smoke was relatively light or dense and if the smoke was continuously present. In many cases the smoke was variable, indicating that the concentration of smoke was rapidly changing as the sample was taken.

There was sufficient wind speed during the series of burns to cause the smoke plume to tilt towards the ground. The wind speed and direction varied during the burns and the interaction of the wind with obstructions near the pan and the fire plume resulted in unquantified disturbances to the air flowing across and around the pan. As a result, the smoke plume would intermittently plunge towards the ground during the burns exposing instrumentation immediately downwind of the pan to gases and particulate in the smoke plume. Further, ground vortices were occasionally observed originating near the pan and moving downwind along the ground. Figure 6 shows the wind driven smoke plume for burn 1106 as normally it would be expected to be rising from the pan driven in the downwind direction. Figure 7 shows one of the intermittent excursions of the smoke plume to ground level during burn 1106 submerging instrumentation in a portion of the smoke plume. This resulted in smoke frequently being visible at ground level at the two downwind measurement locations. There is excellent correlation between the measured CO_2 concentrations and the observations in that the higher measured concentrations correspond

to the observations of denser smoke (figure 7). Further, when clear conditions were observed the measured CO_2 concentrations correspond to the background readings (figure 6). For burns 1103 and 1105 CO_2 concentrations were measured upwind at 45 and 30 m respectively. No smoke was observed at the upwind locations and the CO_2 concentrations remained at the background level. Upwind measurements were not made for the remaining burns so that additional measurements could be made at the downwind locations.

The measurements and observations lead to the conclusion that concentrations of CO_2 above background are only found at ground level when the smoke is observed at ground level. That is to say that elevated levels of CO_2 were only found in the smoke plume.

4.5 Downwind smoke plume trajectory observation

The mesoscale burning experiments have provided the opportunity for scientists at NIST and other laboratories to study the near field environment surrounding an in situ burn of crude oil by making measurements in the area surrounding the pan. Since the burn facilities are located on an island, there is limited downwind distance that can be sampled from the island. In all of the mesoscale tests ground based measurements from the island have been limited to 45 m distance downwind. Video images of the smoke plume 3.5 km from the island provided a quantitative measurement of the plume trajectory downwind for approximately 2 km.

In an effort to obtain qualitative information about the appearance of the plume downwind of the burn, during experiment 1105, observers followed the plume from the burn as it traveled downwind using a USCG HH865 "Dolphin" helicopter. At a distance of 10 km from the pan the head of the smoke plume could just be detected by eye against a sky with broken grey clouds. At the time when the head of the plume was at 10 km from the pan the smoke plume extended back towards the pan for 6 km, figure 8. Based on the 900 seconds duration of fully involved burning for that fire and the measured average wind speed of 9.6 m/s during the burn from Table 4, the expected smoke plume length would be 8.5 km. The observed 6 km length is consistent with this estimate considering the possible variations in wind speed with altitude and distance downwind of the test site. As measured from the helicopter, the nominal depth of the smoke plume was 300 m with a varying width of 0.8 km to 1.6 km.

The smoke plume from a similar mesoscale burn, 1107, was photographed extensively as it traveled downwind from the island. These photographs are shown in figures 9 through 12. In figure 9, the black smoke is emitted from the burn and travels downwind. Figure 10 is 60 s after fire extinction showing the smoke plume as viewed from the rear as it moves downwind. One might also note that some private observers seen in the lower right of the photograph just offshore in a small boat from which they viewed the burn. Figure 11 shows the plume at 500 s after extinction and figure 12 at approximately 1200 s after extinction. At this time the smoke plume, even viewed along its greatest depth from the end on presents only a slight darkening of the background grey sky.

5.0 CONCLUSIONS

In the mesoscale experiments, the wind speed did not appear to affect the average burning rate but did contribute to variations in burning extinction. The recommended value to use for the burning rate of large thick layers of fresh Louisiana crude oils on water is 0.052 ± 0.002 kg/s/m^2 (5.4 ± 0.2 gal/hr/ft^2).

It was generally found that well over 90 percent of the fresh oil was consumed in the pan burns. In addition, the residue from the primary burn could be corralled and burned with the addition of kerosene as an ignitor.

Although smoke yield depends on fire diameter, the smoke yield value of $11 \pm 1\%$ represents most of the mesoscale measurements for fresh Louisiana crude oil.

The size distributions of aerodynamic effective diameters for the smoke particulate show that approximately 80 % of the particulate mass from a 17.2 m effective diameter mesoscale fire was below 10 μm in diameter as measured with a cascade impactor.

Concentrations of CO_2 above background were only found at ground level when the smoke was observed at ground level. That is to say that elevated levels of CO_2 were only found in the smoke plume.

6.0 ACKNOWLEDGEMENTS

This work was funded by the Technology Assessment and Research Program for Offshore Minerals Operations, Minerals Management Service, U.S. Department of the Interior, managed by John Gregory and Ed Tennyson.

The cooperation and support of the U.S. Coast Guard Research and Development Center made the use of the mesoscale burn site possible. The Environmental Safety Branch, under the direction of Commander Pete Tebeau provided funding for operation of the mesoscale test site and Dave Beene of the Marine Fire and Safety Research Branch and the Fire and Safety Test Detachment in Mobile provided outstanding assistance in preparing for and conducting the mesoscale burn experiments.

Donation of crude oil for the experiments was made by the Marine Industry Group (MIRG) through Ron Benton of Shell Oil Company, chairman (MIRG) and the Marine Spill Response Corporation (MSRC) through Jim Simmons provided for the transportation of the crude oil from Louisiana to Mobile and the deliveries to the mesoscale burn site.

J. Randall Lawson, Jay McElroy, Roy McLane and Robert Vettori of the Building and Fire Research Laboratory, NIST provided immeasurable assistance in conducting the mesoscale burns.

Appreciation is extended to the U.S. Coast Guard Aviation Training Center for providing a helicopter and crew which made aerial observations of the plume possible.

7.0 REFERENCES

1. Smith, N.K. and Diaz, A., In-place burning of Prudhoe Bay Oil in broken ice. Proceedings 1985 Oil Spill Conference, Prevention, Behavior, Control, Cleanup. pp. 405-410, 1985.

2. Tennyson, E.J., Results from Selected Oil Spill Response Research by the Minerals Management Service - Marine Technology Society Journal Volume 24 Number 4, pp 27-32, 1990

3. Brown, H.M. and Goodman, R.H., "In Situ Burning of Oil in Ice Leads," Proceedings of the Ninth Annual Arctic and Marine Oilspill Program Technical Seminar, June 10-12, 1986, Edmonton, Alberta, Canada, Environment Canada, Ottawa K1A 0H3, pp. 245-256, 1986.

4. Buist, I.A., and Twardus, E.M., "Burning Unconfined Oil Slicks: Large Scale Tests and Modelling," Proceedings of the Eighth Annual Arctic Marine Oilspill Program Technical Seminar, June 18-20, 1985, Edmonton, Alberta, Canada, Environment Canada, Ottawa K1A 0H3, pp. 103-130, 1985.

5. Evans, D., Baum, H., McCaffrey, B., Mulholland, G., Harkleroad, M., and Manders, W., "Combustion of Oil on Water," Proceedings of the Ninth Arctic Marine Oilspill Program Technical Seminar, June 10-12, 1986, Edmonton, Alberta, Ministry of Supply and Services Canada Cat. No. En 40-11/5-1986E, pp. 301-336, 1986.

6. Evans, D., Mulholland, G., Gross, D., Baum, H., and Saito, K., "Environmental Effects of Oil Spill Combustion," Proceedings of the Tenth Arctic and Marine Oilspill Program Technical Seminar, June 9-11, 1987, Edmonton, Alberta, Ministry of Supply and Services Canada Cat. No. En 40-11/5-1987E, pp. 91-130, 1987.

7. Evans, D., Mulholland, G., Gross, D., Baum, H., and Saito, K., "Burning, Smoke Production, and Smoke Dispersion from Oil Spill Combustion," Proceedings of the Eleventh Arctic and Marine Oil Spill Program Technical Seminar, June 7-9, 1988, Vancouver, British Columbia, Ministry of Supply and Services Canada, Cat. No. En 49-11/5-1988 E/F, pp. 41-87, 1988.

8. Evans, D., Baum, H., Mulholland, G., Bryner, N., and Fomey, G., "Smoke Plumes From Crude Oil Burns," Proceedings of the Twelfth Arctic and Marine Oil Spill Program Technical Seminar, June 7-9, 1989, Calgary, Alberta, Ministry of Supply and Services Canada, Cat. No. En 40-11/5-1989, pp. 1-22, 1989.

9. Evans, D., Walton, W., Baum, H., Lawson, R., Rehm, R., Harris, R., Ghoniem, A., Holland, J., "Measurement of Large Scale Oil Spill Burns," Proceedings of the Thirteenth Arctic and Marine Oil Spill Program Technical Seminar, June 6-8, 1990, Edmonton, Alberta, Ministry of Supply and Services Canada, Cat. No. En 40-11/5-1990. pp. 1-38, 1990.

10. Benner, B. A. Jr., Bryner, N. P., Wise, S. A., Mulholland, G. W., Lao, R. C., Fingas, M. F., "Polycyclic Aromatic Hydrocarbon Emissions from the Combustion of Crude Oil on Water," Environmental Sciences & Technology, Vol. 24, pp. 1418-1427, 1990.

11. Evans, D., Walton, W., Baum, H., Mulholland, G., Lawson, J., Koseki, H., Ghoniem, "Smoke Emission from Burning Crude Oil," Proceedings of the Fourteenth Arctic and Marine Oil Spill Program Technical Seminar, June 12-14, 1991, Vancouver, British Columbia, Ministry of Supply and Services Canada, Cat. No. En 40-11/5-1991. pp. 421-449, 1991.

12. Evans, D., Tennyson, E.J., In-Situ Burning -- A Promising Oil Spill Response Strategy, Seventh Symposium on Coastal and Ocean Management, July 8-12, 1991, Long Beach, California, conference preprint, 1991.

13. Evans, D., Walton, W., Baum, H., Notarianni, K., Lawson, J., Tang, H., Keydel, K., Rehm, R., Madrzykowski, D., Zile, R., Koseki, H., and Tennyson E., "In-Situ Burning of Oil Spills: Mesoscale Experiments," Proceedings of the Fifteenth Arctic and Marine Oil Spill Program Technical Seminar, June 10-12, 1992, Edmonton, Alberta, Ministry of Supply and Services Canada, Cat. No. En 40-11/5-1992. pp. 593-657, 1992.

14. Walton, W., Evans, D., McGrattan, K., Baum, H., Twilley, W., Madrzykowski, D., Rehm, R., Koseki, H., and Tennyson E., "In-Situ Burning of Oil Spills: Mesoscale Experiments and Analysis," Proceedings of the Sixteenth Arctic and Marine Oil Spill Program Technical Seminar, June 7-9, 1993, Calgary, Alberta, pp. 679-734, 1993.

15. Hering, S.V. (editor), Air Sampling Instruments for Evaluation of Atmospheric Contaminates, 7th Edition, American Conference of Governmental Industrial Hygienists, Cincinnati, Ohio, 1989.

16. Marple Personnel Cascade Impactors, Series 290, Instrument Manual, Bulletin No. 290I.M.-3-82, Sierra Instruments, Inc, Carmel Valley, CA.

17. Walton, W., "In Situ Burning of Oil Spills: Mesoscale Experiments," National Institute of Standards and Technology, Gaithersburg, MD, NISTIR, to be published.

Table 1. Burn size

Burn No.	Burn Size (m)	Burn Area		Effective Burn Diameter		Burn Area/ Full Pan Area (%)	Features
		(m^2)	(ft^2)	(m)	(ft)		
1103	6.10 × 6.10	37.2	400	6.88	22.6	16	boom formed two sides of burn area
1105	15.2 × 15.2	231	2490	17.2	56.4	100	
1106	15.2 × 15.2	231	2490	17.2	56.4	100	
1107	15.2 × 15.2	231	2490	17.2	56.4	100	
1109	15.2 × 15.2	231	2490	17.2	56.4	100	
1110	15.2 × 15.2	231	2490	17.2	56.4	100	

Table 2. Airborne samples

Burn No.	Miniblimp		Start Time (s)	Total Time (s)	Range (m)	Altitude (m)
	No.	Sample				
1103	1	Smoke yield	92	1227	70	30
	2	Smoke yield	317	1002		
1105	1	Smoke yield	60	1200	90	90
1106	1	Smoke yield	50	1099	90	80
1107	1	Smoke yield	23	1235	80	140
	2	Smoke yield	23	1235		
1109	1	Smoke yield	49	1050	40	220
	2	Smoke yield	49	1050		
	3	Smoke yield	609	490		
1110	1	Smoke yield	41	1508	80	110
	2	Smoke yield	41	1508		
	3	Impactor	41	1508		

Note: All times from ignition

Table 3. Ground meteorological conditions

Burn No.	Temp. (°C)		Wind Speed (m/s)		Wind Direction (degrees)		Relative Humidity (%)		Barometric Pressure (kPa)		Solar Radiation (kW/m²)
1103 avg.	25.5	24.8	4.1	4.5	171	165	76	76	101.0	101.6	0.70
Minimum	25.2	24.7	2.9	3.2	39	138	73	76	101.0	101.5	0.69
Maximum	25.7	25.1	5.1	6.1	188	187	78	77	101.0	101.6	0.71
1105 avg.	10.7	10.2	4.7	5.0	340	341	69	76	101.4	101.7	0.35
Minimum	10.5	10.0	2.9	3.1	11	27	66	74	101.4	101.7	0.17
Maximum	11.1	10.7	7.0	8.7	269	299	73	78	101.4	101.8	0.79
1106 avg.	11.8	11.3	3.8	3.8	340	339	48	50	102.0	102.3	0.59
Minimum	11.2	10.5	1.8	0.8	20	33	44	48	101.9	102.3	0.14
Maximum	12.5	11.6	6.4	7.0	284	245	53	53	102.0	102.5	0.65
1107 avg.	12.9	12.4	3.6	4.1	3	358	43	46	102.3	102.7	0.62
Minimum	12.6	11.9	2.0	2.5	36	38	41	45	102.2	102.7	0.44
Maximum	13.2	13.0	5.2	7.1	314	322	45	47	102.3	102.8	0.76
1109 avg.	20.3	20.4	2.1	2.2	16	12	55	57	102.1	102.6	0.24
Minimum	19.9	19.9	0.9	0.7	52	41	52	56	102.1	102.6	0.06
Maximum	20.5	20.7	2.8	3.4	342	338	59	57	102.2	102.6	0.56
1110 avg.	19.3	19.2	1.9	2.9	100	100	69	71	102.2	102.6	0.19
Minimum	19.1	18.3	0.4	1.3	19	55	68	69	102.2	102.5	0.15
Maximum	19.6	19.7	3.3	4.6	197	130	71	73	102.2	102.6	0.21

Table 4. Airborne meteorological conditions

Burn No.	Temp. (°C)	Wind Speed (m/s)	Wind Direction (degrees)
1103 avg.	25.9	7.8	179
Minimum	25.7	6.4	167
Maximum	26.1	8.7	190
1105 avg.	9.0	9.6	352
Minimum	8.7	6.2	39
Maximum	9.4	12.6	260
1107 avg.	10.8	5.7	337
Minimum	10.2	3.2	0
Maximum	11.6	8.6	313
1109 avg.	18.3	3.2	53
Minimum	17.9	1.1	16
Maximum	18.6	4.3	97
1110 avg.	17.7	4.9	82
Minimum	17.6	3.6	63
Maximum	17.9	6.5	101

1106 - Not available

Table 5. Burn chronology

Burn No.	Effective Burn Dia. (m)	Initial Oil Depth (mm)	Time to Full Involvement (s)	Time to Begin Boiling (s)	Time to Begin Extinction (s)	Time to Extinction (s)
1103	6.88	61	92	720	1104	1334
1105	17.2	57	180	825	1080	1158
1106	17.2	56	90	730	938	3620
1107	17.2	54	102	627	857	1177
1109	17.2	54	80	600	965	990
1110	17.2	55	91	666	911	1530

Note: All times from ignition

Table 6. Oil volume

Burn No.	Crude		Residue		Consumed		Consumed (%)	Residue burns
	(m^3)	(gal)	(m^3)	(gal)	(m^3)	(gal)		
1103	2.26	596	0.02	5	2.24	591	99	none
1105	13.1	3460	0.09	25	13.0	3435	99	1st - 3000 s
1106	12.9	3415	0.11	30	12.8	3385	99	none
1107	12.6	3320	0.09	25	12.6	3295	99	1st - 1440 s
1109	12.5	3290	0.28	75	12.5	3215	98	1st - 1320 s 2nd - 1140 s
1110	12.7	3350	0.28	75	12.7	3275	98	1st - 1140 s 2nd - 360 s

Note: Residue quantities after residue burns if applicable

Table 7. Water Properties

Burn Number	Salt Concentration (% NaCl)	Specific Gravity
1103	0.84	1.007
1105	0.75	1.006
1106	0.76	1.006
1107	0.74	1.006
1109	0.71	1.005
1110	0.67	1.005

Table 8. Burning rate

Burn No.	Effective Burn Dia. (m)	Burn Time (s)	Burning Rate			Surface Regression Rate (mm/s)
			($kg/s/m^2$)	(kW/m^2)	MW	
1103	6.88	1012	0.053	2210	82	0.062
1105	17.2	900	0.054	2240	520	0.063
1106	17.2	848	0.053	2235	515	0.063
1107	17.2	755	0.051	2120	490	0.060
1109	17.2	885	0.052	2180	505	0.061
1110	17.2	820	0.050	2095	485	0.059

Table 9. Burning rate (customary units)

Burn No.	Effective Burn Dia. (ft)	Burn Time (s)	Initial Oil Thickness (in)	Burning Rate ($gal/hr/ft^2$)	Surface Regression Rate (in/min)
1103	22.6	1012	2.4	5.50	0.15
1105	56.4	900	2.2	5.60	0.15
1106	56.4	848	2.2	5.55	0.15
1107	56.4	755	2.2	5.30	0.15
1109	56.4	885	2.1	5.45	0.15
1110	56.4	820	2.2	5.20	0.14

Table 10. Oil surface regression rate

Burn No.	Effective Burn Dia. (m)	Surface Regression Rate from Pressure Transducer Measurements (mm/s)	Surface Regression Rate from Liquid Level Measurements (mm/s)
1103	6.88	0.062	0.060
1105	17.2	0.063	0.062
1106	17.2	0.063	0.065
1107	17.2	0.060	0.071
1109	17.2	0.061	0.059
1110	17.2	0.059	0.065

Table 11. Smoke yield

Burn No.	Effective Burn Dia. (m)	Sample	Start Time[1] (s)	Total Time (s)	Smoke Yield (%)
1103	6.88	1	92	1227	14.0
		2	317	1002	15.2
1105	17.2	1	60	1200	10.3
1106	17.2	1	50	1099	11.1
1107	17.2	1	23	1235	10.4
		2	23	1235	9.9
1109	17.2	1	49	1050	9.4
		2	49	1050	9.6
		3 - boiling	609	490	11.2
1110	17.2	1	41	1508	12.3
		2	41	1508	11.2

1 - Times from ignition

Table 12. Cascade impactor stage cutpoint size diameters

Stage 1 (μm)	Stage 2 (μm)	Stage 3 (μm)	Stage 4 (μm)	Stage 5 (μm)	Stage 6 (μm)	Stage 7 (μm)	Stage 8 (μm)	Back-up Filter
21.3	14.8	9.8	6.0	3.5	1.55	0.93	0.52	0

Table 13. Water temperature for burns 1103 and 1105

	Burn Number 1103 6.88 m effective diameter				Burn Number 1105 17.2 m effective diameter			
	4066 s before ignition		After extinction time n/a		6690 s before ignition		850 s after extinction	
	North	West	North	West	North	South	North	South
Elevation (mm)	Water temperature (°C)				Water temperature (°C)			
surface (elevation mm)	23.1 (470)	22.9 (485)	24.2 (470)	26.5 (485)	15.9 (485)	15.8 (495)	18.1 (465)	45.0[1] (470)
460	22.8	22.6	24.6	25.6	16.0	16.0	17.5	48.3[1]
380	23.0	22.4	24.7	25.0	16.4	16.0	16.7	20.4
305	22.8	22.3	24.4	24.7	16.1	16.4	16.6	16.9
230	22.9	22.4	24.8	24.8	16.3	16.3	16.3	16.7
150	22.7	22.3	27.9	24.5	16.2	16.1	16.4	16.5
75	22.8	22.3	24.9	24.5	16.2	16.1	16.5	16.5
bottom	22.5	22.4	24.8	24.0	16.1	16.5	16.5	16.5

1 - in oil residue

Table 14. Water temperature for burns 1106 and 1107

	Burn Number 1106 17.2 m effective diameter				Burn Number 1107 17.2 m effective diameter			
	8240 s before ignition		745 s after extinction		5700 s before ignition		1520 s after extinction	
	North	South	North	South	North	South	North	South
Elevation (mm)	Water temperature (°C)				Water temperature (°C)			
surface (elevation mm)	11.9 (465)	11.3 (465)	18.5 (460)	14.3 (450)	12.2 (460)	11.9 (460)	17.8 (460)	55.5[1] (460)
460	12.3	12.2	-	-	-	-	-	-
380	12.2	12.8	14.2	14.2	12.4	12.7	14.8	17.9
305	12.0	12.4	13.9	14.3	12.3	12.7	13.6	12.8
230	12.0	12.7	13.7	14.2	12.4	12.6	13.0	12.9
150	12.4	12.7	13.2	14.3	12.0	12.8	13.0	12.7
75	12.5	12.4	13.3	14.3	12.4	13.0	12.9	12.8
bottom	12.7	12.3	13.7	14.3	13.0	13.0	13.2	13.0

Table 15. Water temperature for burns 1109 and 1110

	Burn Number 1109 17.2 m effective diameter				Burn Number 1110 17.2 m effective diameter			
	7650 s before ignition		1260 s after extinction		6260 s before ignition		1210 s after extinction	
	North	South	North	South	North	South	North	South
Elevation (mm)	Water temperature (°C)				Water temperature (°C)			
surface (elevation mm)	15.6 (470)	16.7 (470)	42.2 (465)	68.4[1] (480)	18.3 (480)	18.4 (480)	53.1 (480)	59.0[1] (480)
460	15.0	15.8	34.5	53.9[1]	18.1	17.7	41.8	44.5
380	15.0	15.8	16.1	16.5	18.1	18.0	18.0	18.2
305	14.8	15.2	15.9	16.5	17.9	17.7	17.8	18.2
230	15.0	15.5	15.4	16.1	18.1	18.0	17.8	18.2
150	15.1	14.7	15.2	16.4	18.1	17.7	17.9	18.0
75	15.3	14.7	15.2	18.5	18.2	18.1	17.8	18.2
bottom	15.4	14.4	15.1	16.4	18.5	17.8	17.7	18.2

1 - in oil residue

Table 16. Ground Level CO_2 Concentration for Burn 1103

24 m Downwind			32 m Downwind		
Time (s)	CO_2 (ppm)	Observations	Time (s)	CO_2 (ppm)	Observations
-1246	338	background	-1126	338	background
14	342	light smoke	74	342	light smoke
314	442	dense smoke	434	395	dense smoke
734	419	dense smoke	854	357	dense smoke
1154	482	dense smoke	1214	402	dense smoke
1274	371	light smoke	1334	337	light smoke

Table 17. Ground Level CO_2 Concentration for Burn 1105

30 m Downwind			45 m Downwind		
Time (s)	CO_2 (ppm)	Observations	Time (s)	CO_2 (ppm)	Observations
-3870	345	background	-3810	344	background
30	381	light smoke	90	366	variable smoke
330	519	dense smoke	390	358	variable smoke
630	348	variable smoke	750	345	variable smoke
930	348	variable smoke	990	349	variable smoke
1050	349	light smoke	1170	362	light smoke
1230	342	clear	1290	343	clear

Table 18. Ground Level CO_2 Concentration for Burn 1106

30 m Downwind			45 m Downwind		
Time (s)	CO_2 (ppm)	Observations	Time (s)	CO_2 (ppm)	Observations
-1155	354	background	-1275	356	background
45	351	clear	105	355	clear
225	362	variable smoke	285	349	clear
405	651	dense smoke	465	367	variable smoke
585	382	variable smoke	645	395	variable smoke
765	379	variable smoke	825	369	light smoke
885	465	variable smoke	1005	357	light smoke
1065	376	light smoke	1125	357	light smoke
1245	385	variable smoke	1305	361	light grass smoke
1425	357	clear	1485	353	light grass smoke
3705	358	clear	3765	349	clear

Table 19. Ground Level CO_2 Concentration for Burn 1107

30 m Downwind			45 m Downwind		
Time (s)	CO_2 (ppm)	Observations	Time (s)	CO_2 (ppm)	Observations
-363	355	background	-303	357	background
-3	353	light smoke	57	350	light smoke
177	382	variable smoke	237	368	variable smoke
297	392	light smoke	417	353	variable light smoke
537	367	variable smoke	597	358	light smoke
657	393	dense smoke	777	360	variable smoke
837	350	variable smoke	897	351	variable light smoke
957	346	variable light smoke	1017	347	clear
1137	349	light smoke	1197	342	clear
1317	351	clear	1377	344	clear

Table 20. Ground Level CO_2 Concentration for Burn 1109

30 m Downwind			45 m Downwind		
Time (s)	CO_2 (ppm)	Observations	Time (s)	CO_2 (ppm)	Observations
-630	349	background	-552	348	background
30	349	light smoke	90	350	clear
167	350	variable light smoke	235	352	clear
300	353	clear	359	377	clear
445	349	clear	518	343	clear
603	355	light grass smoke	670	340	clear
739	351	very light smoke	807	342	clear
885	350	clear	960	344	clear
1023	346	clear	1082	342	clear
1155	343	clear	1258	343	clear

Table 21. Ground Level CO_2 Concentration for Burn 1110

30 m Downwind			45 m Downwind		
Time (s)	CO_2 (ppm)	Observations	Time (s)	CO_2 (ppm)	Observations
-1129	344	background	-1029	347	background
6	344	clear	64	344	clear
131	357	light smoke	198	345	clear
266	348	light grass smoke	334	345	light smoke
418	349	light smoke	491	349	clear
557	352	light smoke	626	346	clear
696	353	light smoke	761	342	light grass smoke
821	349	variable light smoke	881	340	clear
936	348	light smoke	1001	347	clear
1067	353	light smoke	1141	342	clear
1586	344	clear	1656	344	clear

Figure 1. 15.2 m square mesoscale crude oil burn

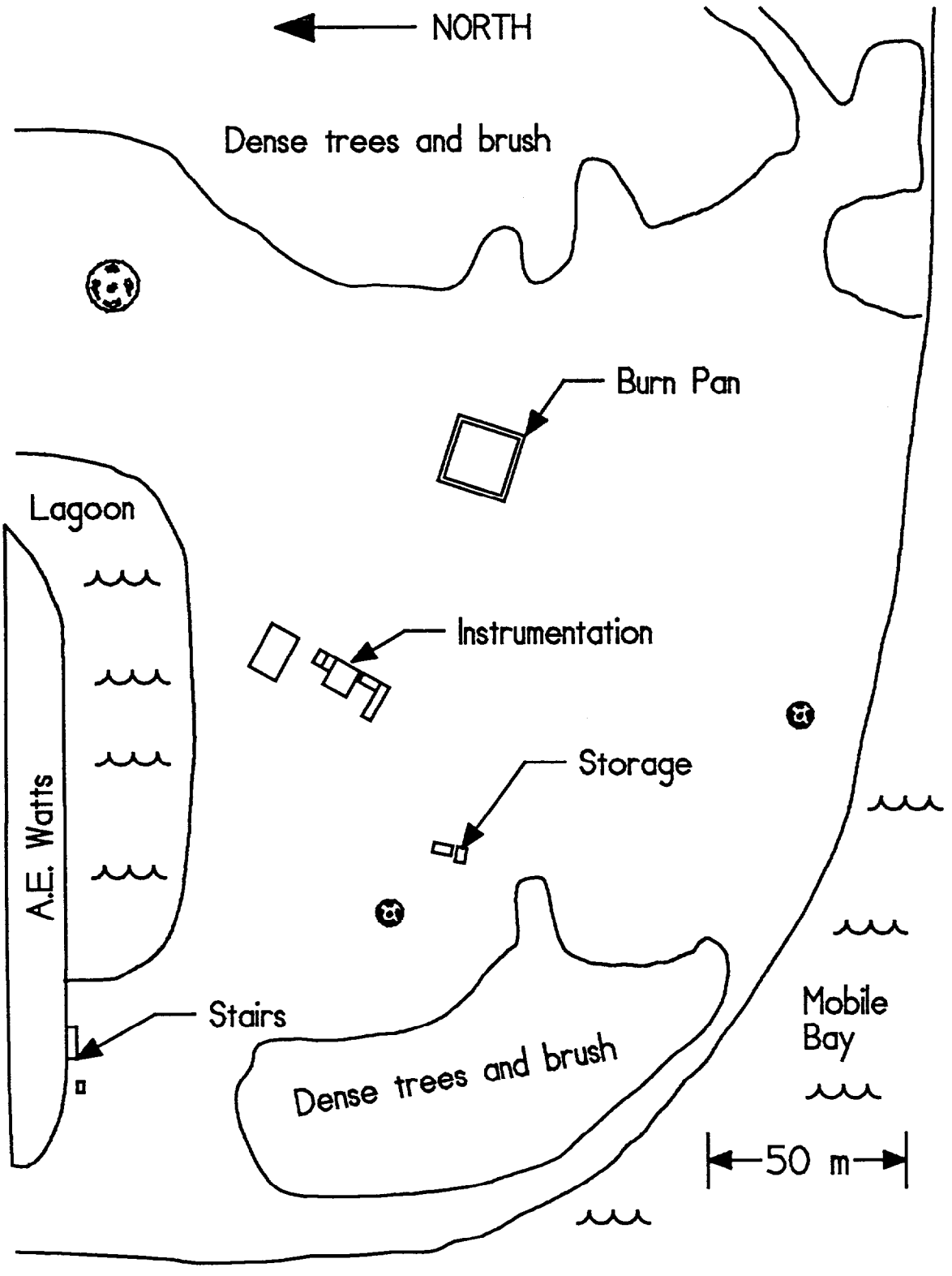

Figure 2. USCG mesoscale burn facility site plan

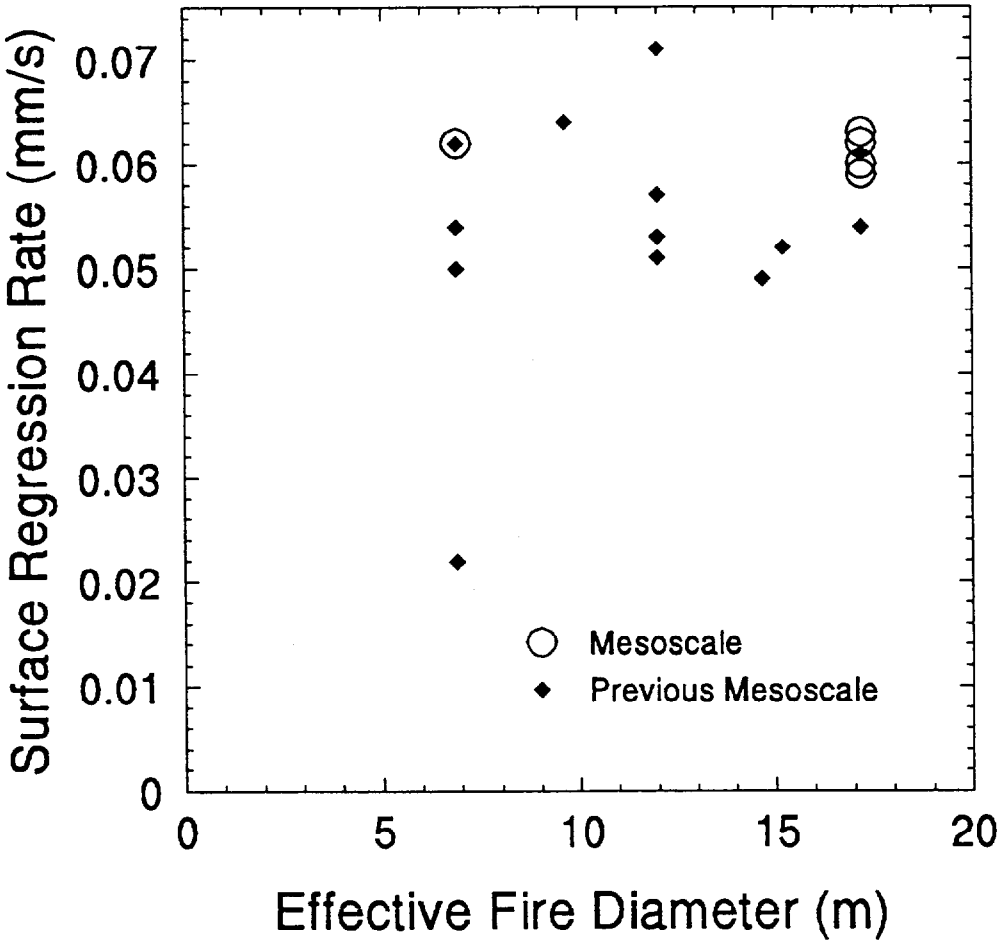

Figure 3. Crude oil surface regression rate

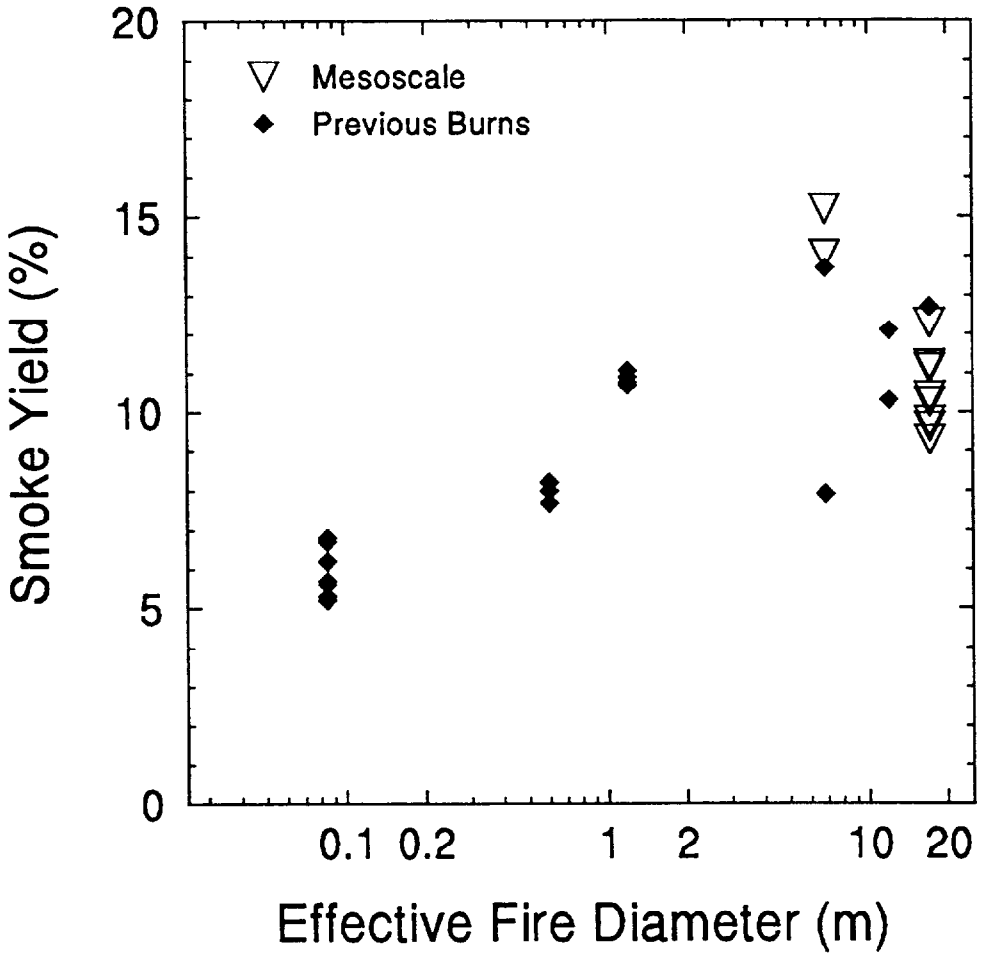

Figure 4. Smoke yield

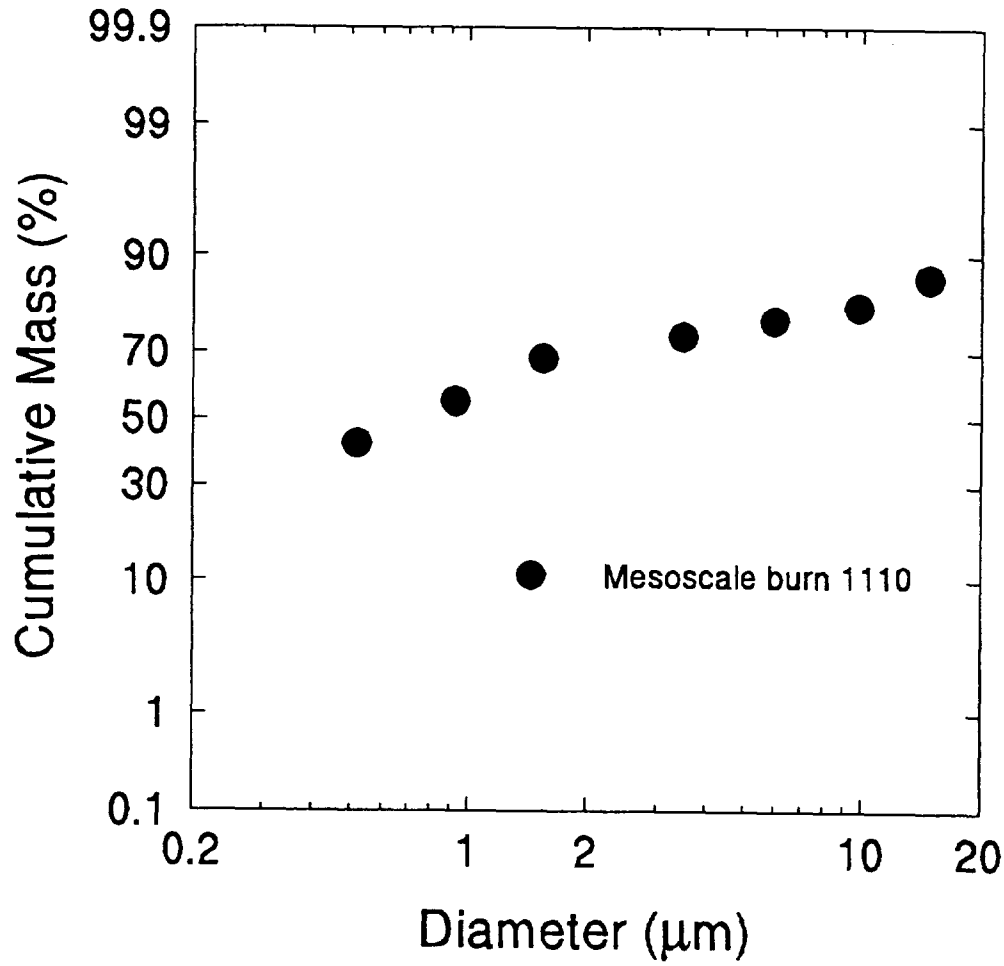

Figure 5. Smoke particulate cumulative size distribution for mesoscale burn 1110

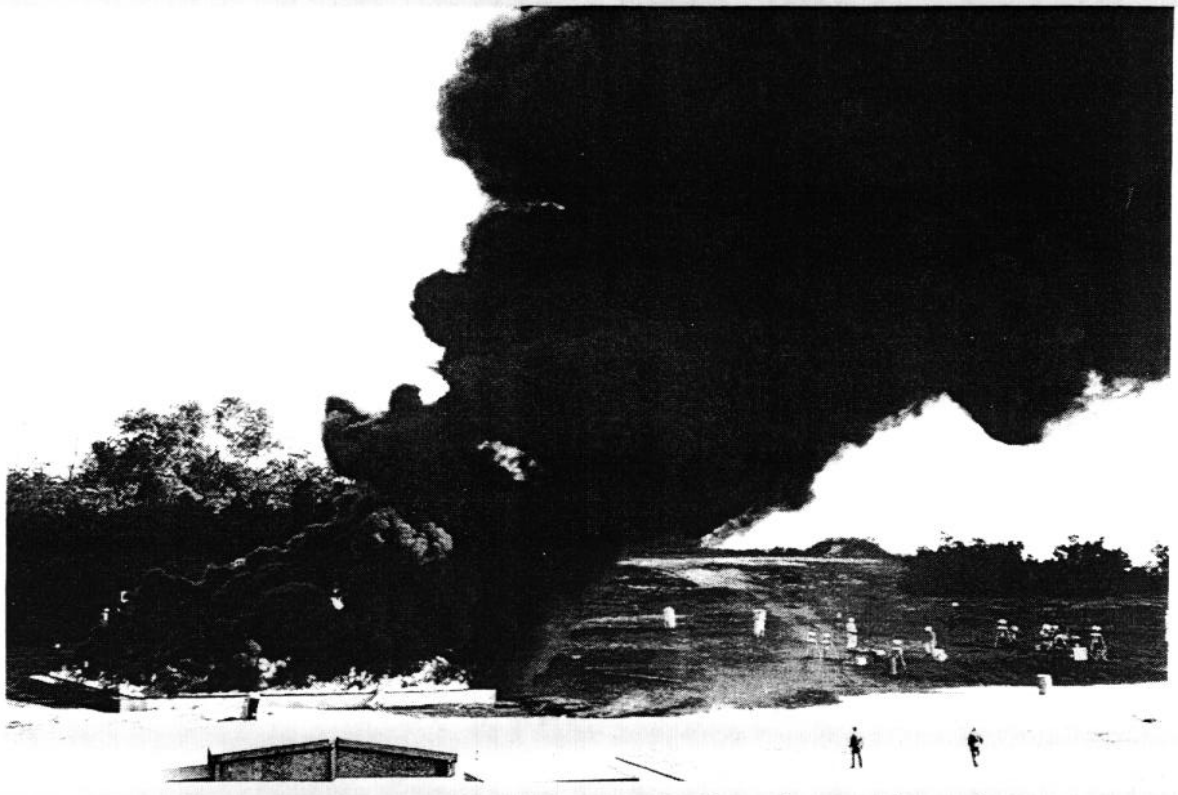

Figure 6. Mesoscale burn 1106 with smoke above the ground near the pan

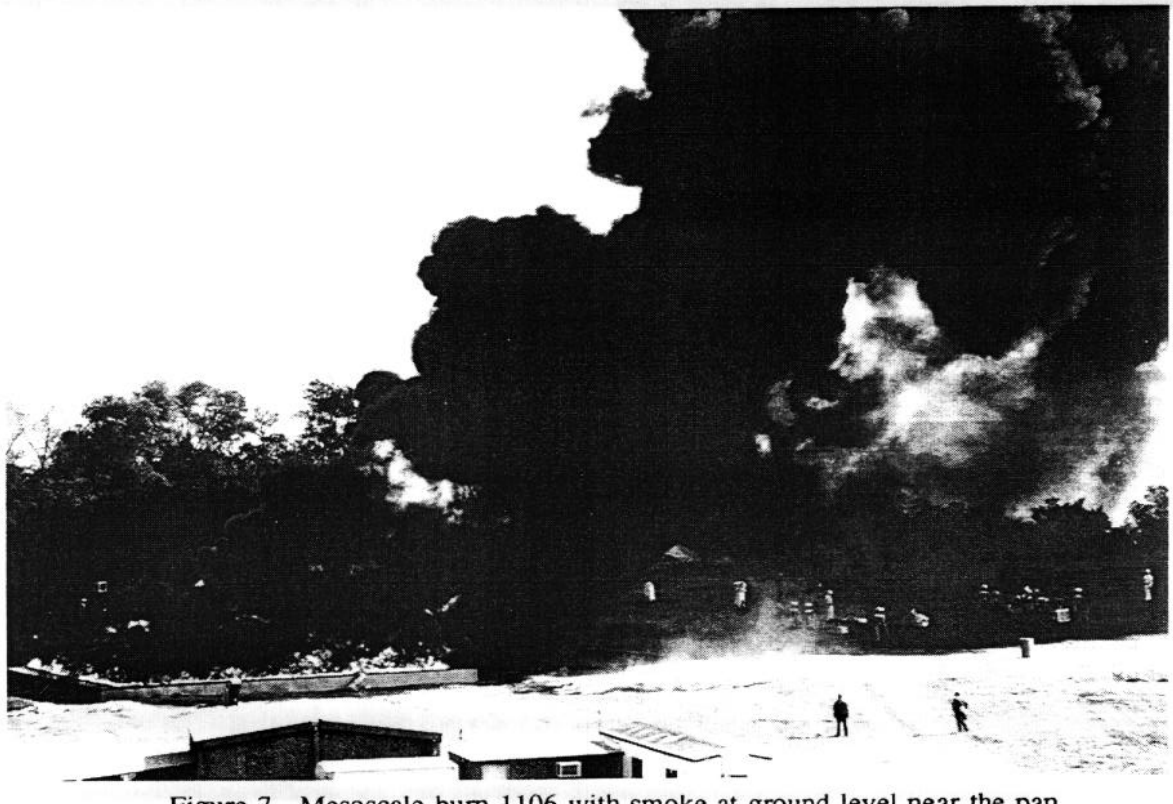

Figure 7. Mesoscale burn 1106 with smoke at ground level near the pan

Figure 8. Smoke plume from mesoscale burn 1105 as viewed from helicopter approximately 10 km downwind looking upwind towards the test site

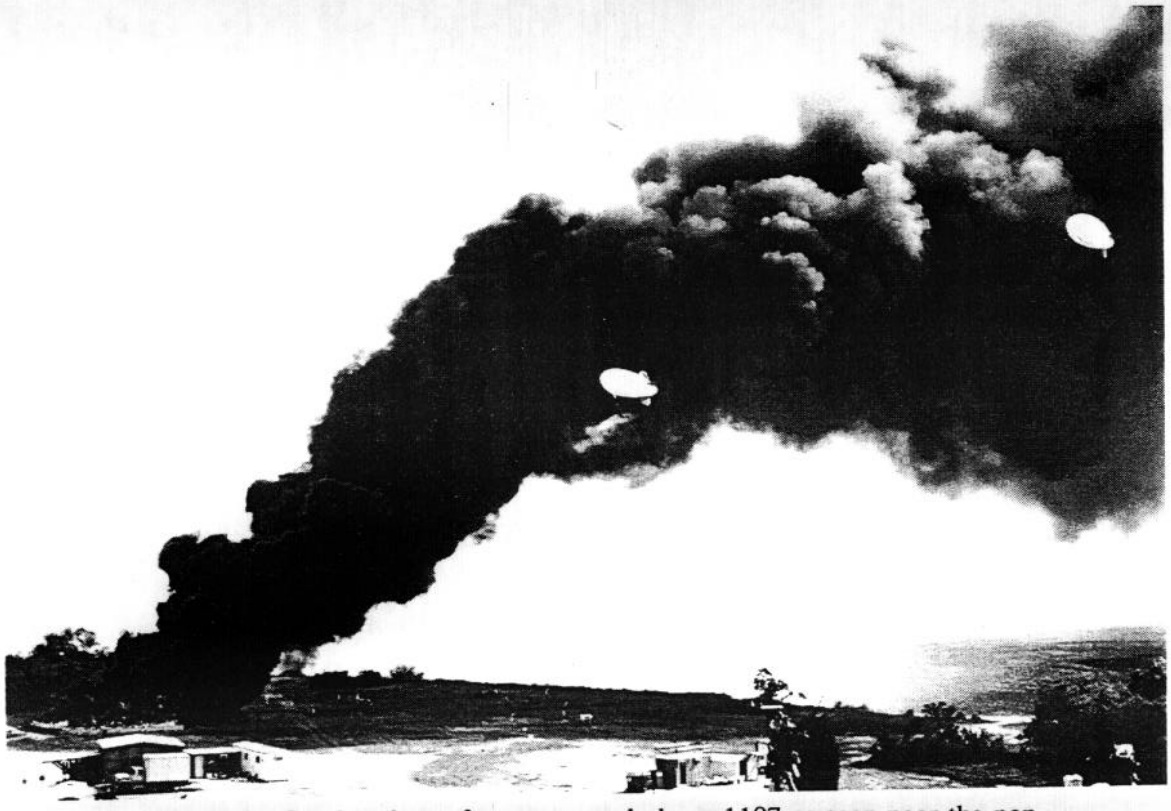

Figure 9. Smoke plume from mesoscale burn 1107 as seen near the pan

Figure 10. Smoke plume from mesoscale burn 1107 moving downwind 60 s after extinction as viewed from the test site

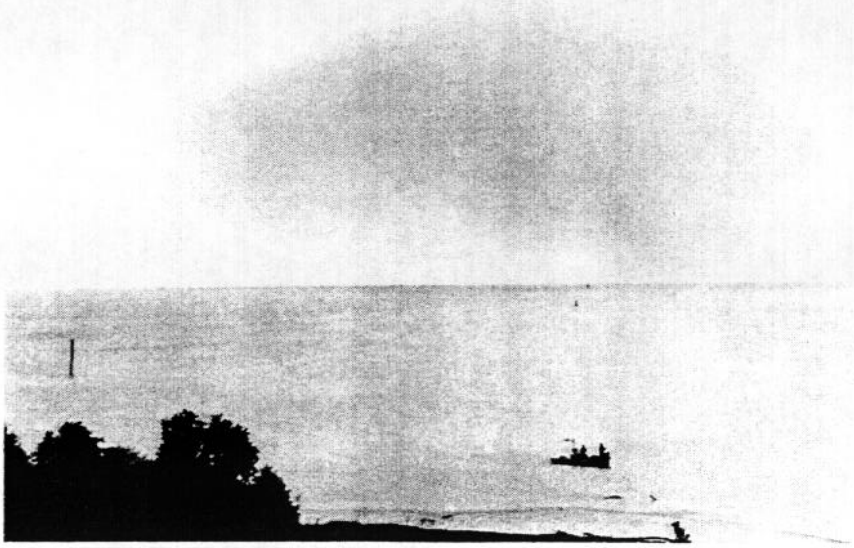

Figure 11. Smoke plume from mesoscale burn 1107 moving downwind 500 s after extinction as viewed from the test site

Figure 12. Oval shaped smoke plume from mesoscale burn 1107 appears near the horizon 1200 s after extinction as viewed from the test site

NIST-114
(REV. 6-93)
ADMAN 4.09

U.S. DEPARTMENT OF COMMERCE
NATIONAL INSTITUTE OF STANDARDS AND TECHNOLOGY

MANUSCRIPT REVIEW AND APPROVAL

(ERB USE ONLY)
ERB CONTROL NUMBER | DIVISION
PUBLICATION REPORT NUMBER | CATEGORY CODE
PUBLICATION DATE | NUMBER PRINTED PAGES

INSTRUCTIONS: ATTACH ORIGINAL OF THIS FORM TO ONE (1) COPY OF MANUSCRIPT AND SEND TO THE SECRETARY, APPROPRIATE EDITORIAL REVIEW BOARD.

TITLE AND SUBTITLE (CITE IN FULL)
In Situ Burning of Oil Spills: Mesoscale Experiments and Analysis

CONTRACT OR GRANT NUMBER

TYPE OF REPORT AND/OR PERIOD COVERED

AUTHOR(S) (LAST NAME, FIRST INITIAL, SECOND INITIAL)
Walton, W. D.

PERFORMING ORGANIZATION (CHECK (X) ONE BOX)
[X] NIST/GAITHERSBURG
[ ] NIST/BOULDER
[ ] JILA/BOULDER

LABORATORY AND DIVISION NAMES (FIRST NIST AUTHOR ONLY)
Building and Fire Research Laboratory (864)

SPONSORING ORGANIZATION NAME AND COMPLETE ADDRESS (STREET, CITY, STATE, ZIP)
U.S. Department of Interior
Minerals Management Service
Technology Assessment and Research Branch
Herndon, VA 22070

PROPOSED FOR NIST PUBLICATION

[ ] JOURNAL OF RESEARCH (NIST JRES)	[ ] MONOGRAPH (NIST MN)	[ ] LETTER CIRCULAR
[ ] J. PHYS. & CHEM. REF. DATA (JPCRD)	[ ] NATL. STD. REF. DATA SERIES (NIST NSRDS)	[ ] BUILDING SCIENCE SERIES
[ ] HANDBOOK (NIST HB)	[ ] FEDERAL INF. PROCESS. STDS. (NIST FIPS)	[ ] PRODUCT STANDARDS
[ ] SPECIAL PUBLICATION (NIST SP)	[ ] LIST OF PUBLICATIONS (NIST LP)	[ ] OTHER _____
[ ] TECHNICAL NOTE (NIST TN)	[X] NIST INTERAGENCY/INTERNAL REPORT (NISTIR)	

PROPOSED FOR NON-NIST PUBLICATION (CITE FULLY) [ ] U.S. [ ] FOREIGN

PUBLISHING MEDIUM
[X] PAPER [ ] CD-ROM
[ ] DISKETTE (SPECIFY) _____
[ ] OTHER (SPECIFY)

SUPPLEMENTARY NOTES

ABSTRACT (A 2000-CHARACTER OR LESS FACTUAL SUMMARY OF MOST SIGNIFICANT INFORMATION. IF DOCUMENT INCLUDES A SIGNIFICANT BIBLIOGRAPHY OR LITERATURE SURVEY, CITE IT HERE. SPELL OUT ACRONYMS ON FIRST REFERENCE.) (CONTINUE ON SEPARATE PAGE, IF NECESSARY.)

A series of six mesoscale experiments were performed to measure the burning characteristics of Louisiana crude oil on water in a pan. These included one - 6 m square and five - 15 m square burns. Results of the measurements for burning rate and smoke emissions are compared to those from previous burns of various scales. The burning rate as indicated by the regression rate of the oil surface was found to be 0.062 ± 0.003 mm/s for both the 6 m and 15 m square pan fires. Smoke particulate yields from the 15 m square fires were found to be approximately 11% of the oil burned on a mass basis.

KEY WORDS (MAXIMUM OF 9; 28 CHARACTERS AND SPACES EACH; SEPARATE WITH SEMICOLONS; ALPHABETIC ORDER; CAPITALIZE ONLY PROPER NAMES)
burning rate, crude oil, fire tests, heat release rate, oil spills, particle size distribution, plumes, smoke yield

AVAILABILITY
[X] UNLIMITED [ ] FOR OFFICIAL DISTRIBUTION - DO NOT RELEASE TO NTIS
[ ] ORDER FROM SUPERINTENDENT OF DOCUMENTS, U.S. GPO, WASHINGTON, DC 20402
[X] ORDER FROM NTIS, SPRINGFIELD, VA 22161

NOTE TO AUTHOR(S): IF YOU DO NOT WISH THIS MANUSCRIPT ANNOUNCED BEFORE PUBLICATION, PLEASE CHECK HERE. [ ]

ELECTRONIC FORM